



# Demographic models predict end-Pleistocene arrival and rapid expansion of pre-agropastoralist humans in Cyprus

Corey J. A. Bradshaw<sup>a,b,1</sup> , Christian Reepmeyer<sup>b,c,d,2</sup> , Frédéricik Saltré<sup>a,b</sup> , Athos Agapiou<sup>e</sup> , Vasiliki Kassianidou<sup>f</sup>, Stella Demesticha<sup>g</sup> , Zomenia Zomeni<sup>g</sup> , Miltiadis Polidorou<sup>h</sup> , and Theodora Moutsiou<sup>d,f,1,2</sup>

Edited by Melinda Zeder, Smithsonian National Museum of Natural History, Washington, DC; received October 19, 2023; accepted April 9, 2024

The antiquity of human dispersal into Mediterranean islands and ensuing coastal adaptation have remained largely unexplored due to the prevailing assumption that the sea was a barrier to movement and that islands were hostile environments to early hunter-gatherers [J. F. Cherry, T. P. Leppard, *J. Isl. Coast. Archaeol.* 13, 191–205 (2018), [10.1080/15564894.2016.1276489](https://doi.org/10.1080/15564894.2016.1276489)]. Using the latest archaeological data, hindcasted climate projections, and age-structured demographic models, we demonstrate evidence for early arrival (14,257 to 13,182 calendar years ago) to Cyprus and predicted that large groups of people (~1,000 to 1,375) arrived in 2 to 3 main events occurring within <100 y to ensure low extinction risk. These results indicate that the postglacial settlement of Cyprus involved only a few large-scale, organized events requiring advanced watercraft technology. Our spatially debiased and Signor–Lipps-corrected estimates indicate rapid settlement of the island within <200 y, and expansion to a median of 4,000 to 5,000 people (0.36 to 0.46 km<sup>-2</sup>) in <11 human generations (<300 y). Our results do not support the hypothesis of inaccessible and inhospitable islands in the Mediterranean for pre-agropastoralists, agreeing with analogous conclusions for other parts of the world [M. I. Bird *et al.*, *Sci. Rep.* 9, 8220 (2019), [10.1038/s41598-019-42946-9](https://doi.org/10.1038/s41598-019-42946-9)]. Our results also highlight the need to revisit these questions in the Mediterranean and test their validity with new technologies, field methods, and data. By applying stochastic models to the Mediterranean region, we can place Cyprus and large islands in general as attractive and favorable destinations for paleolithic peoples.

archaeology | carrying capacity | human expansion | maritime movements | paleolithic

Maritime mobility is an essential component of human migration and the development of an interconnected, globalized world. While there is convincing evidence of the Pleistocene occupation of island landscapes in the Caribbean (1), insular Southeast Asia (2, 3), and North Asia (4) following an intensification of maritime movements (5, 6), Pleistocene peopling of the Mediterranean region is still strongly debated (7–10). Although a locus of important migration and transmission routes, a pre-agropastoralist peopling of Cyprus is often dismissed because of the assumption that the Mediterranean Sea was a barrier to all early human sea movements (11) and that islands in the region were too unproductive to have sustained nonagricultural societies (12).

One argument for the later occurrence of island peopling and maritime mobility in the eastern Mediterranean compared to Southeast Asia, for example, derives from biogeographic differences between tropical and Mediterranean latitudes. Phoca-Cosmetatou and Rabett (13) proposed that a paucity of maritime resources due to a lack of reef formation in the eastern Mediterranean stalled the emergence of specialized maritime communities observed in Southeast Asia. Arguments have emerged that the initial establishment on islands occurred only during the terminal Pleistocene associated with the climate reversal in the Younger Dryas (YD) (10). During that period, environmental productivity declined and forced hunter-gatherers into more mobile subsistence systems that included the adaptation of more advanced maritime technologies (14). However, research on the pattern of obsidian exploitation and transportation in the eastern Mediterranean indicates that initial maritime crossings appeared earlier at a minimum of 15,000 y ago (15).

Cyprus' location in the eastern Mediterranean is at the nexus of important migration and innovation routes because of its proximity to the Fertile Crescent in the Near East, and its visibility from many points on the continent (16). Although Cyprus was never connected to the mainland, sea crossings from the neighboring Levantine coast would have involved navigating distances as little as 30 to 70 km depending on the episode of marine regression (16). Hunter-gatherer populations occupied the surrounding mainland since at least 1.4 Ma (1 Ma = 1 My B.P.) (17–21), and these populations were adapted to coastal living and

## Significance

Because of persisting narratives of isolation, inaccessibility, and “unattractiveness”, the initial peopling of one of the eastern Mediterranean islands is commonly regarded as a Neolithic (agro-pastoralist) phenomenon, initiated by farming populations from the mainland following demographic pressures. We show instead that Cyprus could have been permanently peopled by hunter-gatherer populations by around 14 to 13 thousand years ago, earlier than previously accepted. We also showed that this process must have involved few, large migration events (100s to 1,000s of people) that infer the intent and organization of these early humans. Our results enhance our understanding of the timing, and the climatic and demographic conditions influencing the initial peopling of Cyprus, with potential implications for other Mediterranean islands.

The authors declare no competing interest.

Copyright © 2024 the Author(s). Published by PNAS. This article is distributed under [Creative Commons Attribution-NonCommercial-NoDerivatives License 4.0 \(CC BY-NC-ND\)](https://creativecommons.org/licenses/by-nc-nd/4.0/).

Although PNAS asks authors to adhere to United Nations naming conventions for maps (<https://www.un.org/geospatial/mapsgeo>), our policy is to publish maps as provided by the authors.

This article is a PNAS Direct Submission.

<sup>1</sup>To whom correspondence may be addressed. Email: [corey.bradshaw@flinders.edu.au](mailto:corey.bradshaw@flinders.edu.au) or [moutsiou.theodora@ucy.ac.cy](mailto:moutsiou.theodora@ucy.ac.cy).

<sup>2</sup>C.R. and T.M. contributed equally to this work.

This article contains supporting information online at <https://www.pnas.org/lookup/suppl/doi:10.1073/pnas.2318293121/-DCSupplemental>.

Published May 16, 2024.

maritime travel, aided by visibility of Cyprus from certain continental locations during the Late Pleistocene (45 to 12 ka; 1 ka = 1,000 y B.P.) (16, 22).

Cyprus is the third largest island of the Mediterranean, with sufficient productivity to support large human populations, so it provides an important case study to investigate the timing and nature of the initial peopling of island systems in the Late Pleistocene. There is a persistent yet unfounded assumption that island discovery and occupation in the Late Pleistocene were random processes, especially considering that there is no remaining evidence of watercraft from so long ago (23). However, modeling suggests instead that the initial peopling of islands in much earlier periods (more than 60 ka) must have involved extensive and well-planned expeditions to ensure sufficiently large founding groups that could have established persistent, long-term populations (e.g., refs. 2 and 24).

In this paper, we first estimated the probable first entry of people into Cyprus based on a stochastic Signor–Lipps correction to a calibration of the accepted radiocarbon time series. We then applied this window of arrival in a stochastic demographic model to estimate the minimum founding population of hunter-gatherers required to

persist indefinitely. Our demographic model of hunter-gatherers is predicated on carrying capacity estimated from hindcasting climate models [HadCM3 (Hadley Centre Coupled Model version 3) including the BIOME4 vegetation model] (25). Our results show strong support for the hypothesis of an early arrival during the Late Pleistocene of large groups of people and a rapid west–east expansion within a few hundred years.

Results

**Estimated Entry Window.** The ten oldest dates from sites spread across Cyprus (Fig. 1) ranged from  $11,720 \pm 240$  (lab ID: Beta-40380) to  $8,470 \pm 50$  (lab ID: Beta-256039)  $^{14}\text{C}$  (radiocarbon) years B.P., which is calibrated to  $13,640 \pm 0.281$  ka to  $9,483 \pm 0.430$  ka based on the IntCal20 calibration curve (26). Applying the calibrated resampled inverse-weighted McNerney (CRIWM) algorithm (27) to correct for the “Signor–Lipps effect”, we obtain a plausible window of entry ranging from 14,257 to 13,182 ka (Fig. 1). This window therefore predates the onset of the YD by at least 300 y, and the onset of the Holocene by at least 1,100 y (Fig. 1).

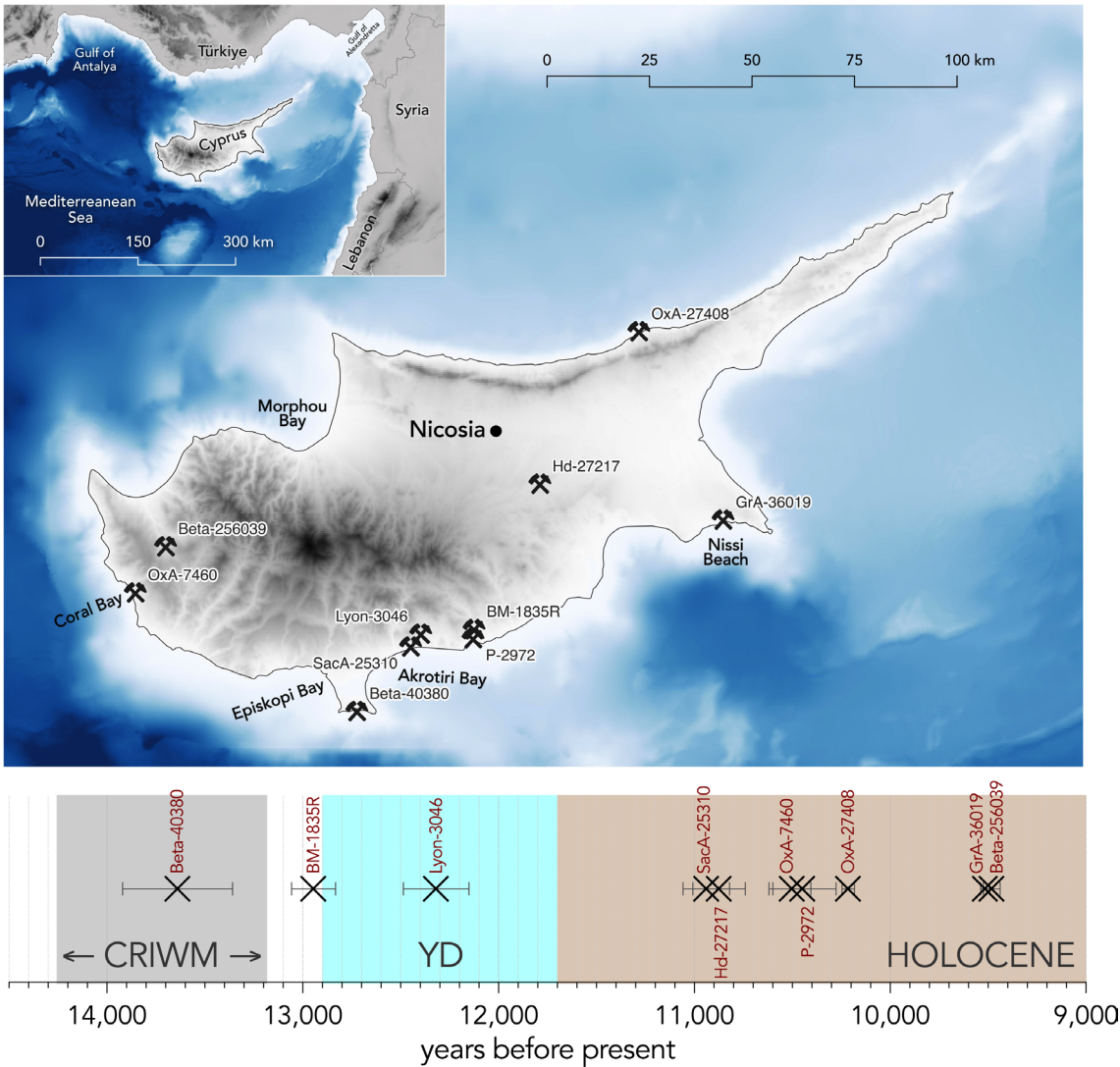


**Fig. 1.** Location of oldest dated archaeological sites (Top), with CRIWM (27) estimate of the initial entry window (gray shading). Also shown are the duration of the YD (blue shading) and the early Holocene (brown shading). Background blue gradient represents relative bathymetry. Archaeological date IDs and their sites of origin (in brackets) are OxA-27408 (Akanthou Arkosyko), Hd-27217 (Ayia Varvara Asprokremnos), GrA-36019 (Nissi Beach), BM-1835R (Kalavassos Ayios Dhimitrios/Ayious), P-2972 (Kalavassos Tenta), Lyon-3046 (Parekklesia Shillouroukambos), SacA-25310 (Ayios Tychonas Klimonas), Beta-40380 (Akrotiri Aetokremnos), OxA-7460 (Kissonerga Mylouthkia), and Beta-256039 (Kritou Marottou Ais Yiorkis).



**Fig. 2.** Spatially debiased pattern of expansion inferred from data in the Near East Radiocarbon Date database (31). Scale bar shown in years relative to initial entry. Sites with names shown as crossed hammers. Background blue gradient represents relative bathymetry. The truncation of the earliest dates in the southwest is a necessary outcome of the similarity in dates from sites in the southwest, implying occupation of that section of the island within years, compared to a slower (decades to a century) occupation to the northeast beyond the Troodos Mountains.

Applying a spatial debiasing algorithm (28) to the available archaeological dates, a dominant southwest-to-northeast pattern of establishment emerges (Fig. 2). Another feature revealed is the rapid establishment across all parts of the island in <200 y (6 to 7 human generations) from initial arrival (Fig. 2), which appears realistic considering the size of the island (~maximum 240 km east–west, and 100 km north–south). This produces a maximum occupation rate of  $1.4 \text{ km y}^{-1}$ , which is comparable to the maximum movement rates estimated for Sahul <65 ka ( $\sim 0.4 \text{ km y}^{-1}$ ) (29) and 0.5 to  $0.9 \text{ km y}^{-1}$  estimated for migration across Eurasia after permanent movement out of Africa (30).

**Hindcasted Climate Conditions.** Anomalies of the hindcasted climate variables derived from the grid cells covering the island of Cyprus show a steady rise in temperature, precipitation, and net primary production from about 18 to 11 ka at the onset of the Holocene (*SI Appendix, Appendix I and Fig. S1*). At 14 ka, the model predicts a net primary production of the grid cells covering Cyprus ranging from  $181$  to  $223 \text{ g C m}^{-2} \text{ y}^{-1}$ , whereas other sites with dated archaeological material around 14 ka on the mainland (e.g., Karain and Öküzini Caves, Türkiye; Moghr El Ahwal Cave 3, Lebanon; Hayonim Terrace and Kebara Cave, Israel) have hindcasted net primary production ranging from  $140$  to  $216 \text{ g C m}^{-2} \text{ y}^{-1}$  (*SI Appendix, Appendix I and Fig. S2*).

**Minimum Viable Founding Population Size.** Progressively increasing the founding population size from 500 to 4,000 people, we identified the lower asymptotic probability of quasiextinction at approximately 0.11 (Fig. 3), which corresponds to around 2,750 people as the estimate of minimum viable founding population size (Fig. 3). The probability of quasiextinction continues to

decline beyond 2,750 people, but at a much lower rate (i.e., an instantaneous exponential rate of change  $[r] \gtrsim -0.03$ ) compared to when the founding population is <2,750 (i.e.,  $r \lesssim -0.03$ ; Fig. 3).

**Demographic Projections.** With a single entry of 2,750 people on average between 14,257 and 13,182 y ago, the population could have grown to as many as ~10,000 (upper 95% confidence limit) in as few as 320 y (median = 4,122; lower 95% confidence limit = 505) (Fig. 4). The median population size varied between ~4,000 and 5,000 people (i.e.,  $0.36$  and  $0.46 \text{ people km}^{-2}$ ) during the YD and >5,000 by the onset of the Holocene (Fig. 4).

Dividing the minimum viable population size into smaller units identified that the probability of quasiextinction remained high up to  $0.38N$  (i.e., 1,045 people), which translates to around 2 or 3 main immigration events ranging in size between ~1,000 to 1,375 people arriving within a period of 6 to 98 y (Fig. 5). This does not necessarily imply that each event was a single, mass migration of ~1,000 people arriving simultaneously; rather, a more likely scenario is that smaller family groups arrived in high-frequency waves within the time frames predicted by our model.

## Discussion

In the Mediterranean, persisting narratives posit that the regional insular landscape was largely inhospitable to mobile hunter-gatherer groups, who presumably preferred the more extensive continental territories with their diverse and robust biotas (7, 10, 11). In this context, hunter-gatherers are hypothesized to have been reluctant to exploit islands due to the “unattractiveness” (7) of the insular landscape and did not exploit islands until agropastoralism,



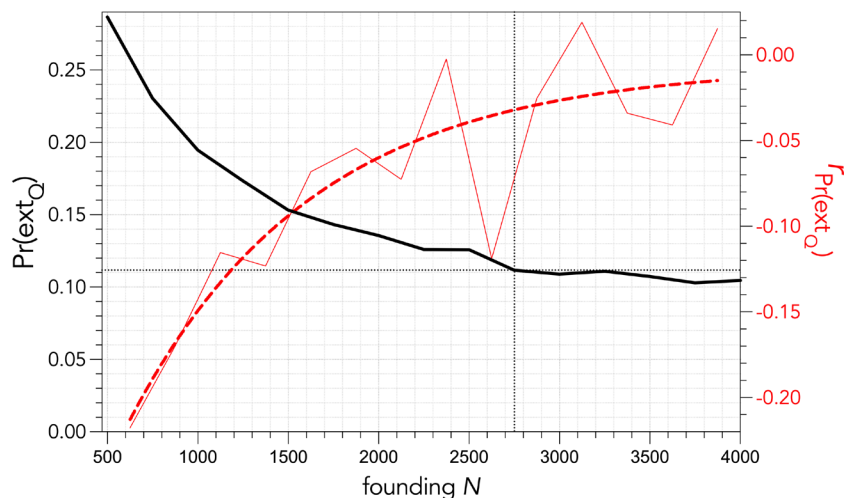


**Fig. 3.** Estimated probability of quasiextinction (declining <50 people; black line, *Left y axis*), and the instantaneous exponential rate of change ( $r$ ) of the quasiextinction probability  $\text{Pr}(\text{ext}_Q)$  (red line, *Right y axis*), for different starting population sizes (founding population  $N$ ), where  $r = \log_e(\text{Pr}(\text{ext}_Q)_{t+1}/\text{Pr}(\text{ext}_Q)_t)$ . The dashed red line is an exponential plateau model of the form  $\hat{y} = y_{\max} - (y_{\max} - y_0)e^{-kx}$ , where  $y_{\max} = 0.104$ ,  $y_0 = 0.439$ , and the rate constant  $k = 0.001259$ , applied to smooth the  $r$  trajectory to show the central trend.

and the introduction of cereals, pulses, and ovicaprids, provided a viable strategy to establish human communities on the Mediterranean islands. It has been argued that human dispersal to and occupation of Cyprus and other eastern Mediterranean islands is implicitly or explicitly attributed to demographic pressures on the mainland in the wake of abrupt climatic change that forced farming populations to move to new areas out of necessity rather than choice as coastal areas were inundated by postglacial sea-level rise (7, 32).

This interpretation is a consequence of major gaps in the archaeological record of Cyprus, deriving from differential preservation of archaeological material, taphonomic biases, uncertainties associated with dating, and limited DNA evidence. The difficulty of locating sites of that timeframe on Cyprus is also directly associated with the island's eroding landscape (33). Discerning the plausible demographic conditions of human arrival to Cyprus therefore requires an alternative approach.

The combination of our Signor–Lipps-corrected window of initial human entry at 14,257 to 13,182 y ago, the inference of human carrying capacity derived from the HadCM3 climate model (25), and our resulting demographic model predictions definitively do not support the hypothesis of Cyprus being “unattractive” to humans

during the late Pleistocene. First, the hindcasted net primary production for Cyprus is similar or higher than the predicted net primary production at major known archaeological sites on the southern coast of Türkiye and the Mediterranean coast of the Levant (*SI Appendix, Appendix I and Fig. S2*). Second, the entry window clearly predates both the YD and the onset of the Holocene (Fig. 1). Even if the earliest date of Akrotiri *Aetokremnos* (a site with a well-established correlation of hippopotamus *Phanourios minor* bones and stone artifacts) (34, 35) is removed, Signor–Lipps correction of the radiocarbon series still places the window of arrival at 12,757 to 13,162 y ago (i.e., firmly into the terminal Pleistocene), prior to the earliest appearance of agro-pastoralist communities on the mainland (22). The estimated entry window of humans into Cyprus falls into a timeframe of substantial environmental change. Fast sea-level rise during Meltwater Pulse 1A and the potentially connected initiation of the Bølling–Allerød Warm Period (36) are clearly visible in the temporally finer-resolution (seamless; cf. HadCM3: 1,000-y increments) TraCE21ka climate model that captures the dynamics of the Bølling–Allerød interstadial and YD better than other global circulation models (37). The TraCE21ka climate model shows an abrupt warming peak just prior to our predicted window of human arrival (*SI Appendix, Appendix I and Fig. S3*). The

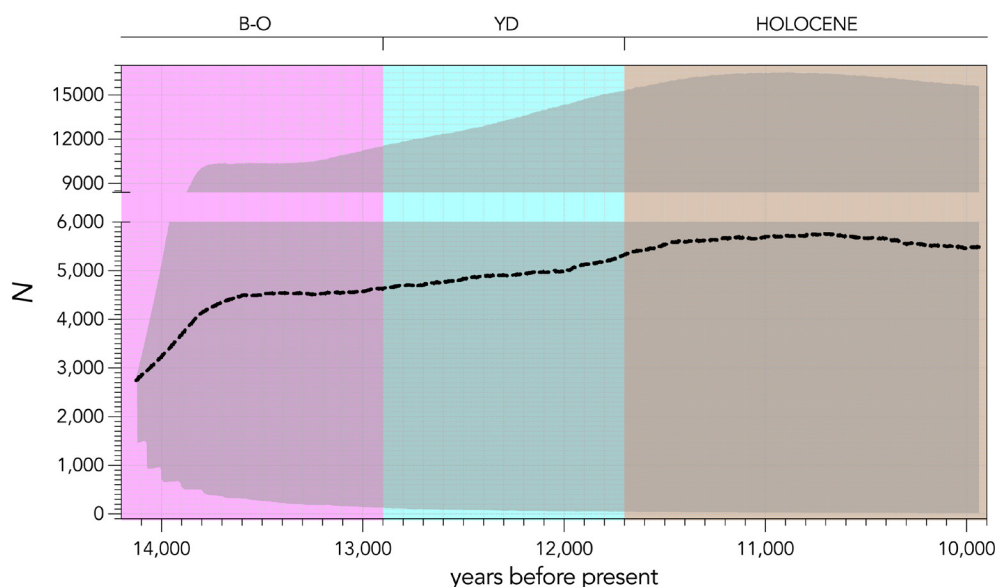


**Fig. 4.** Median (with 95% CI shaded gray) projection of the human population size ( $N$ ) with a starting population of 2,750 people entering the island between 14,257 and 13,182 y ago. Also shown are the Bølling–Allerød interstadial (B–O; light pink shading), the YD (blue shading), and the early Holocene (brown shading).

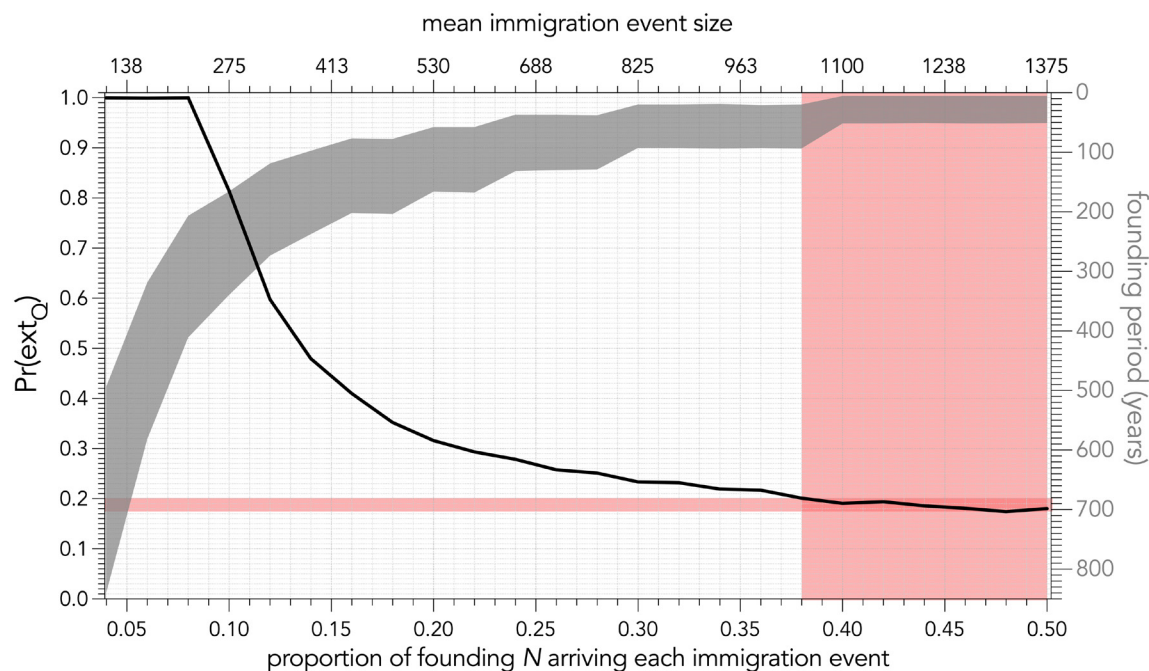


**Fig. 5.** Estimated probability of quasi-extinction  $\Pr(\text{ext}_Q)$  with varying entry population sizes and timings. Starting with a minimum viable population size ( $N$ ) of 2,750, and splitting  $N$  into proportions from 0.04  $N$  to 0.50  $N$  arriving every 5 to 50 y (with the interval itself stochastically resampled), demonstrates that only about 2 to 3 immigration events of ~1,000 to 1,375 people (light red vertical shaded area) each on average arriving within a window of ~6 to 98 y (founding period; Right y axis) minimize quasiextinction probability.

proposed mass migration to Cyprus would therefore coincide with this period of accelerated environmental change (i.e., warmer and wetter than the preceding period).

Third, our projected median population growing to densities of 0.36 to 0.46  $\text{km}^{-2}$  within <300 y (i.e., <11 human generations) is consistent with modeled and inferred density ranges for pre-agropastoralist societies in the European/Near East region (*SI Appendix, Appendix 1* and *Table S1* and associated text). Indeed, a bootstrapped median density of the available estimates provides a range of 0.045 to 0.433 people  $\text{km}^{-2}$  from the entire European/Near East region. Focusing exclusively on the density estimates from the Levant and eastern Mediterranean, a region that was inhabited intensively throughout Marine Isotope Stages 2 (29 ka to 12 ka) and 3 (57 ka to 29 ka) (38), the bootstrapped median density was 0.129 to 1.324 people  $\text{km}^{-2}$ , showing that our estimated densities are well within expectation. But even our density estimates should be considered conservative because they are based entirely on terrestrial resources; the contribution of marine resources would increase these estimates (e.g., ref. 39).

Our modeling supports a hunter-gatherer occupation of Cyprus, evidenced through the dates of Akrotiri *Aetokremnos* that firmly established the first human arrival on Cyprus in the postglacial period (40). Since then, the excavations at *Aetokremnos* have dominated debates of postglacial sites in Cyprus. Later discoveries pertaining to the existence of forager occupation, such as the pre-agropastoralist habitation site in the Troodos foothills, Vretsia *Roudias* (12 ka) (41), support this hypothesis. Ephemeral coastal surface artifact scatters such as Akamas *Aspros* and Nissi Beach are also supporting evidence for a postglacial occupation of Cyprus (42). *Aspros* is important because of its rich lithic assemblage and because it contains the first traces of material recovered offshore during an underwater survey. A second cluster of sites reported by surveys in central Cyprus provides 12 more surface-collected lithic assemblages with analogies to the excavated Akrotiri phase

sites (43, 44). Despite none of these lithic assemblages having dates, the sites demonstrate possible early exploration from the shore to the island's interior via the Tremithous and Yialias river basins (45). Hunting and foraging activities persisted during the development of the first permanent settlements, such as Ayios Tychonas *Klimonas*, demonstrating mixed economies encompassing hunting, plant cultivation, and modest consumption of marine foods at the beginning of sedentary occupation of Cyprus (46).

The assumed direct association of agriculture and sedentism with population growth and migration as a consequence of demographic pressure has recently been challenged, with evidence demonstrating that foraging societies experienced the same high rate of growth as contemporaneous transitioning farming societies across a broad range of geographies, climates, and environments with different carrying capacities (47). Increased access to resources at a new destination is a strong impetus for a rapid expansion to new territories (e.g., ref. 48) that are contra hypotheses of environmental and demographic stress in previously occupied areas as primary factors behind human movement. Indeed, bioenergetic availability influences the number of moves and distances covered in modern hunter-gatherer societies rather than the decision for movement itself (49, 50).

Archaeological and fossil evidence demonstrates that by 45 ka, *Homo sapiens* hunter-gatherer groups had populated western Eurasia (the continental region surrounding Cyprus), occupying multiple ecozones, ranging from tundras in central Siberia to coastal biomes in south-western and Mediterranean regions (16, 51). Our study showcases that hunter-gatherer groups demonstrated the same ecological plasticity in the initial peopling of Cyprus. Further, the available dated material indicates a rapid establishment across the entire island within fewer than 200 y, with a general gradient of movement from the west to the east that approximately follows the precipitation gradient (*SI Appendix, Appendix 1* and *Fig. S4*). Such a speedy occupation of the island would have likely resulted in a rapid

modification of the insular landscape, potentially impacting the availability of subsistence resources (e.g., mammalian fauna) (9, 40).

This southwest–northwest pattern of expansion might seem to contradict results from virtual passive drift-modeling that identified more support for paths to the northern coast of Cyprus from the southern coast of Türkiye compared to paths from northern locations in the Levant (52). However, there are several considerations that limit the relevance of comparing passive drifting and the terrestrial expansion patterns our models revealed for Cyprus following initial human arrival. First, the passive-drift models all had a low probability of reaching Cyprus, regardless of departure point ( $<0.06$ ), and even the moderately more successful paths from southern Türkiye are not associated with any relevant archaeological sites dating to the late Epipaleolithic/early Neolithic period from which to define plausible departure points (52). Second, the available drift-model results are contingent on passive drifting, whereas our results support larger-scale crossings that would have required both active propulsion and directionality, similar to the inferences made for island-chain crossings from Wallacea to Sahul much earlier (2). Third, it is important to understand that we are modeling *occupation* processes (i.e., sufficient human presence to leave behind discoverable and datable archaeological material), and not just temporary movement through an area (e.g., ref. 30), so even if initial arrivals were predominately on the northern coast of Cyprus, later occupation of the more favorable western region could have precipitated more archaeological evidence of the earliest human presence. Regardless, the essential result of the spatially debiased spread model is the rate of occupation, not the directionality per se. Further, additional archaeological dates from the poorly sampled regions of Cyprus might eventually reveal alternative expansion patterns and taphonomic biases in our inferences based on the data currently available.

Without independent data with which to validate model hindcasts, we can only compare the relative probabilities of different modeled scenarios to provide insights into the plausible patterns of the initial occupation of Cyprus. There are other limitations to our inferences in addition to those arising from potential taphonomic biases in the distribution and availability of dated archaeological material. These include the still unknown relationship between hunter-gatherer densities and net primary production as inferred from global circulation models (29, 30). Furthermore, the complexity of vegetation submodels in coupled Earth-systems models are continuously improving, so finer-scale and better-calibrated hindcasts of estimated net primary production could conceivably alter our interpretation of pre-agropastoralist human carrying capacity. Additionally, possible biases in estimates of demographic rates for generic hunter-gatherers could reveal different estimates of minimum viable population size, even though our model predicts population densities and growth rates that agree with both modeled (30) and empirical data (*SI Appendix, Appendix I and Table S1*).

Despite asymptotic behavior of the probability of quasiextinction, there was still a  $\sim 10\%$  that the founding population would go extinct following arrival (hence, the wide CI for the projected population trajectory in Fig. 3). This result is largely driven by the size of the island and the relatively low productivity compared to other regions of the world (e.g., Sahul) (24). Thus, the large founding population we estimated is best viewed as an “insurance policy” against the likelihood of extinction. Our analysis on the frequency of arrivals also supports the idea of large, and by inference, planned migrations to the island. In other words, many small sporadic forays of unconnected people over long periods of time were unlikely to support a permanent population. However, metapopulations (53) of hierarchical groups typical of the complex social networks of hunter-gatherer societies (54) arriving frequently as family groups is another scenario that still fits our model predictions.

In conclusion, we should re-evaluate the dominant hypothesis that islands in the Mediterranean and elsewhere were suboptimal destinations for pre-agropastoralist societies and instead view them as important ecosystems for human expansion. For too long, research on the initial colonization and occupation of islands has remained at the periphery of scientific enquiry, especially in the eastern Mediterranean. By applying stochastic models based on both temporally and spatially explicit data for the first time to the Mediterranean region, we can now place Cyprus as a probable destination for paleolithic peoples.

## Materials and Methods

**Signor–Lipps-Corrected Estimate of Human Arrival.** To hindcast an arrival window that takes into account the low probability of archaeological evidence being preserved and discovered (the Signor–Lipps effect) (55, 56), we accessed the 10 oldest archaeological sites in Cyprus and their oldest dated artifacts (and their SD) from the Near East Radiocarbon Dates database (31). The only site we did not include was Vretsia Roudias because there are no available radiocarbon dates from this site (57); however, there are optically stimulated luminescence dates available for Vretsia Roudias, the oldest of which is  $12.8 \pm 1.6$  ka (*SI Appendix, Appendix II*). To these 10 radiocarbon dates (*Results*), we applied the Rextinct package in R first to calibrate the dates from radiocarbon years to years B.P. based on the IntCal20 Northern Hemisphere calibration curve (26), and then to estimate a Signor–Lipps-corrected window of human arrival using the CRIWM resampling algorithm (27), the most advanced and up-to-date method available that incorporates dating uncertainty in its calculations. The Signor–Lipps correction based on resampling approaches generally requires  $>8$  dates to provide robust estimates of initial or terminal phenomena from dated archaeological or paleontological evidence (58, 59).

To evaluate a spatial gradient of initial arrival across Cyprus from the dated archaeological material, we adapted the spatially debiased Signor–Lipps correction algorithm developed by Saltré et al. (28). Briefly, this maximum-likelihood method, first developed by Solow et al. (60), is adapted to a grid of the island at a spatial resolution of  $\sim 0.01^\circ \times 0.01^\circ$  latitude/longitude (i.e.,  $\sim 1.1$  km  $\times$  1.1 km). For each grid cell, we estimate the age of arrival following a Gaussian probability density function by numerically maximizing the log-likelihood of the calibrated radiometric date series (including their errors). We implemented this approach using the SpatialArrivalEstimates script in R (available at 77). This approach extends to grid cells with and without data, with the latter estimated as a function of the distance of the age relative to the age in a grid cell with data. The approach estimates the spatial bias generated by the model at each grid cell given an optimized bandwidth size (61) and then corrects the spatially explicit estimates of initial appearance by these biases to produce a debiased estimate of initial appearance relative to the first cell occupied.

**Sea Level and Area of Cyprus.** To estimate a human carrying capacity for the island of Cyprus (see next section), first, we required an estimate of the island area as sea levels changed during and following the period of initial human arrival. We first calculated the area of Cyprus relative to estimated 1-m decrements of sea level relative to today (from 0 to  $-130$  m) using the General Bathymetric Chart of the Oceans 2020 (gebco.net;  $15''$  resolution  $\approx 400$  m). We then designed a resampling procedure to link the 1-m sea level intervals in that dataset to the global dated sea level series calculated by Lambeck et al. (62). Taking the Lambert et al. (62) estimates of mean sea-level anomaly (relative to the present) and its SD, we interpolated the series to 1-y intervals using a resampling approach (*SI Appendix, Appendix I and Fig. S5*). Next, we linked the mean (and SD) interpolated sea-level anomalies to the GEBCO 2020 dataset by generating 1,000 random normal deviates of sea level in the time series from 20,000 y ago to the present and then identifying the closest sea level value in the GEBCO dataset to calculate a mean (and SD) area of Cyprus (*SI Appendix, Appendix I and Fig. S5*; relevant code included in the demographic model scripts available in (77)).

**Carrying Capacity.** In the absence of measured compensatory density-feedback mechanisms for ancient humans necessary to constrain the demographic models from projecting a limitless exponential rise (63) (see section below describing the *Demographic Model*), we used a hypothetical reduction in the survival vector by constructing a theoretical carrying capacity ( $K$ ) built from a hindcasted estimates



of net primary production. We used the HadCM3 climate model (25) at the  $0.5^\circ \times 0.5^\circ$  latitude/longitude resolution ( $\sim 55 \text{ km} \times 55 \text{ km}$ ) covering Cyprus from 20 ka to the present to provide estimates of net primary production. HadCM3 is a global circulation model that gives spatially explicit estimates of climate conditions (e.g., mean annual temperature, annual precipitation) and net primary production (based on the BIOME4 vegetation model) (64) every 1,000 y back to 800,000 y ago at a resolution of  $0.5^\circ \times 0.5^\circ$  latitude/longitude. We chose the HadCM3 model because finer temporal-resolution models such as TraCE21ka (65, 66) do not include a vegetation model, and other hindcasting from Earth system models of intermediate complexity such as LOVECLIM (67) are at least partially inadequate for reproducing changes in woody vegetation elsewhere during the Last Glacial Maximum (68).

We isolated the grid cells for Cyprus and extracted the HadCM3 hindcasts of mean annual temperature, mean annual precipitation, and net primary production, as well as their anomalies relative to the present (relevant R code provided in the HadCM3outputs script available in (77)). We chose net primary production ( $\text{g C m}^{-2} \text{ y}^{-1}$ ) as the comprehensive indicator of relative carrying capacity through time (e.g., refs. 24, 29, and 30), translating net primary production into a carrying capacity expressed in units of humans the landscape was capable of supporting. For this, we used the linear relationship between net primary production and human density from Bradshaw et al. (30) that are themselves derived from Tallavaara et al. (69). We chose a linear relationship rather than the nonlinear variants of the human density-net primary production relationships (29, 30) because of the low range of absolute net primary production hindcasted for Cyprus (i.e.,  $<305 \text{ g C m}^{-2} \text{ y}^{-1}$ ) from a global perspective. For each iteration of the demographic model (described below), we generated a times series of carrying capacity that incorporated the variation in net primary production across the grid cells covering Cyprus and the land area of the island (including its uncertainty) (SI Appendix, Appendix I and Fig. S6; relevant code included in the demographic model scripts available in (77)).

**Demographic Model.** We adapted the demographic model from Bradshaw et al. (24) for Pleistocene humans in Sahul (Australia + New Guinea) to the initial Cyprus population to project population trajectories through time. Briefly, that model incorporates realistic demographic rates (survival, fertility, longevity) for hunter-gatherers to parameterize an age-structured projection model. The age-specific survival vector is derived from the five-parameter Siler hazard model (70) based on average "hunter-gatherer" parameter estimates (71). We derived a fertility schedule based on age at primiparity estimates for 22 modern hunter-gatherer groups (72): mean age of female primiparity = 19 y, and total fertility = 4.69 births (i.e., 2.35 daughters) (73).

We applied these estimated demographic rates to a prebreeding,  $81 (i) \times 81 (j)$  element (i.e., 0 to 80 y old) (71) Leslie projection matrix (**M**) for females only, multiplying a population vector **n** to estimate total population size at each forecast time step (74), where total population size =  $2N$  females assuming a 1:1 sex ratio (24). Fertilities ( $m_x$ ) occupy the first row of the matrix, survival probabilities ( $S_x$ ) occupy the subdiagonal, and the diagonal transition probability ( $M_{i,i}$ ) was zero. We projected the **Mn** combinations for each iteration of the simulation to estimate yearly total population size.

To invoke a compensatory density-feedback mechanism that followed the stochastic expression of hindcasted carrying capacity, we multiplied the  $\beta$ -resampled survival vector by 0.98 ( $S_{\text{mod}}$ ). This produces an average 2% drop in average survival each time total abundance exceeds that time step's resampled carrying capacity, thereby lowering the dominant eigenvalue of **M** to  $<0$  (i.e., producing a declining population). We also included a catastrophic die-off function because catastrophic mortality events (C) scale to generation length among vertebrates, where the probability of catastrophe =  $0.14 \text{ generation}^{-1}$  (75) and human generation length was 27.6 y calculated from the deterministic **M** (24). Once invoked at probability C, we halved (binomially resampled) the survival vector to induce a 50% mortality event for that year based on the definition of a catastrophe as "... any 1 y peak-to-trough decline in estimated numbers of 50% or greater" (75). Full model code provided in the CypAspatDemModel script available in (77).

**Stochastic Projections.** We conservatively sampled the start date for each of 10,000 projection iterations using a stochastic uniform sampler between 14,257 and 13,182 y ago, which was the estimated window of arrival from the CRIWM estimate (see Results and approach described in the calibrate script available in (77)). We thus had a different, randomly selected start year for each iteration of the model, to which we projected populations 150 generations into the future (i.e., 4,140 y) based on the stochastically resampled elements of the **M** matrix. To resample survival, we estimated the shape parameters of a  $\beta$  function and then randomly resampled each element of the survival vector for each year of the projection and each iteration of the model (assuming an arbitrary  $\sigma_s = 5\%$  SD of survival). For fertility, we randomly resampled total (female) fertility using a Gaussian model with an arbitrary 5% SD.

**Minimum Viable Founding Population Size.** Using the same model architecture described above, we adjusted the founding population at initial entry from 500 to 4,000 in increments of 250 (i.e., 250 to 2,000 females) to determine the population size where the probability of quasiextinction (Q) began to asymptote (see also ref. 24). We implemented this approach using the CypAspatDemModelMVPsim script available in (77). This threshold is based on the minimum size below which a population cannot avoid inbreeding depression (although the threshold could in fact be much higher) (76). For each increment of founding population size, we repeated the model 10,000 times to estimate a probability of quasiextinction.

**Sequence of Proportional Minimum Viable Population Size.** Estimating a single minimum viable founding population size assumes an instantaneous initial arrival of the entire founding population. This scenario is likely to be less realistic than one where proportions of the founding population arrive in a sequence over some period at a frequency high enough to maintain a low probability of extinction. We therefore designed a second stochastic simulation where we split the minimum viable founding population size into proportions averaging 0.04 to 0.5 (in increments of 0.02), each of which arrived between 5 and 50 y after the previous (using a random uniform sampler) until the full complement of the total minimum viable population size was achieved. Repeating the iteration for each incrementing proportion 5,000 times, we calculated both the probability of quasiextinction as well as the range of total elapsed time from first to final entry (relevant R code available in the script CypAspatDemModelStaggeredEntry script available in (77)). The full code and data repository for all methods and results is available in (77).

**Data, Materials, and Software Availability.** R code & numeric data have been deposited in Zenodo (<https://zenodo.org/records/10951688>) (77).

**ACKNOWLEDGMENTS.** This work was cofinanced by the European Regional Development Fund and the Republic of Cyprus through the Research and Innovation Foundation (EXCELLENCE/0421/0050) for the project Modelling Demography and Adaptation in the Initial Peopling of the Eastern Mediterranean Islandscape (MIGRATE, 2022–2024). Funding provided to C.J.A.B. and F.S. by the Australian Research Council Centre of Excellence for Australian Biodiversity and Heritage (CE170100015).

Author affiliations: <sup>a</sup>Global Ecology | Partuyarta Ngadluku Wardli Kuu, College of Science and Engineering, Flinders University, Adelaide, SA 5001, Australia; <sup>b</sup>Australian Research Council Centre of Excellence for Australian Biodiversity and Heritage, Wollongong, NSW 2522, Australia; <sup>c</sup>Commission for Archaeology of Non-European Cultures, German Archaeological Institute, Bonn 53173, Germany; <sup>d</sup>College of Arts, Society and Education, James Cook University Cairns, Cairns, QLD 4870, Australia; <sup>e</sup>Cyprus University of Technology, Lemesos 3036, Cyprus; <sup>f</sup>Archaeological Research Unit, University of Cyprus, Nicosia 1095, Cyprus; and <sup>g</sup>Geological Survey Department, Ministry of Agriculture, Rural Development and the Environment of the Republic of Cyprus, Nicosia 1301, Cyprus

Author contributions: C.J.A.B., C.R., and T.M. designed research; C.J.A.B., C.R., and T.M. performed research; C.J.A.B., C.R., F.S., Z.Z., and T.M. contributed new reagents/analytic tools; C.J.A.B. and C.R. analyzed data; T.M. funding; and C.J.A.B., C.R., F.S., A.A., V.K., S.D., Z.Z., M.P., and T.M. wrote the paper.

1. F. Saltré et al., Environmental conditions associated with initial northern expansion of anatomically modern humans. *Nat. Commun.* (2024), in press.
2. M. I. Bird et al., Early human settlement of Sahul was not an accident. *Sci. Rep.* **9**, 8220 (2019), 10.1038/s41598-019-42946-9.
3. S. Kealy, J. Louys, S. O'Connor, Reconstructing palaeogeography and inter-island visibility in the Wallacean Archipelago during the likely period of Sahul colonization, 65–45 000 years ago. *Archaeol. Prospect.* **24**, 259–272 (2017), 10.1002/arp.1570.

4. H. Takamiya, M. J. Hudson, H. Yonenobu, T. Kurozumi, T. Toizumi, An extraordinary case in human history: Prehistoric hunter-gatherer adaptation to the islands of the Central Ryukyus (Amami and Okinawa archipelagos), Japan. *The Holocene* **26**, 408–422 (2015), 10.1177/0959683615609752.
5. S. O'Connor, S. Kealy, C. Reepmeyer, S. C. Samper Carro, C. Shipton, Terminal Pleistocene emergence of maritime interaction networks across Wallacea. *World Archaeol.* **54**, 244–263 (2022), 10.1080/00438243.2023.2172072.

6. C. Reepmeyer, S. O'Connor, Mahirta, S. Kealy, T. Maloney, Kisar, a small island participant in an extensive maritime obsidian network in the Wallacean Archipelago. *Archaeol. Res. Asia*. **19**, 100139 (2019), 10.1016/j.ara.2019.100139.
7. T. P. Leppard *et al.*, Global patterns in island colonization during the Holocene. *J. World Prehist.* **35**, 163–232 (2022), 10.1007/s10963-022-09168-w.
8. T. Moutsios, C. Reepmeyer, V. Kassianidou, Z. Zomeni, A. Agapiou, Modelling the Pleistocene colonisation of Eastern Mediterranean islandscapes. *PLoS One* **16**, e0258370 (2021), 10.1371/journal.pone.0258370.
9. A. H. Simmons, *Stone Age Sailors: Palaeolithic Seafaring in the Mediterranean* (Left Coast Press Inc, Walnut Creek, California, USA, 2014).
10. J. F. Cherry, T. P. Leppard, Patterning and its causation in the pre-neolithic colonization of the Mediterranean islands (late Pleistocene to early Holocene). *J. Isl. Coast Archaeol.* **13**, 191–205 (2018), 10.1080/15564894.2016.1276489.
11. C. Broodbank, The origins and early development of Mediterranean maritime activity. *J. Medit. Archaeol.* **19**, 199–230 (2007), 10.1558/jmea.2006.v19i2.199.
12. H. Dawson, *Mediterranean Voyages: The Archaeology of Island Colonisation and Abandonment* (Left Coast Press Inc, Walnut Creek, California, USA, 2014).
13. N. Phoca-Cosmetatou, R. J. Rabett, "Pleistocene Island occupation in the Mediterranean: Insights from a tied-biome approach to glacial refugia" in *Living in the Landscape: Essays in Honour of Graeme Barker*, K. Boyle, R. J. Rabett, C. O. Hunt, Eds. (McDonald Institute for Archaeological Research, University of Cambridge, Cambridge, United Kingdom, 2014), pp. 83–108.
14. A. J. Ammerman, "The first Argonauts: Towards a study of the earliest seafaring in the Mediterranean" in *The Global Origins and Development of Seafaring*, A. Anderson, J. H. Barrett, K. V. Boyle, Eds. (McDonald Institute for Archaeological Research, University of Cambridge, Cambridge, United Kingdom, 2010), pp. 81–92.
15. N. Laskaris, A. Sampson, F. Mavridis, I. Liritzis, Late Pleistocene/Early Holocene seafaring in the Aegean: New obsidian hydration dates with the SIMS-SS method. *J. Archaeol. Sci.* **38**, 2475–2479 (2011), 10.1016/j.jas.2011.05.019.
16. T. Moutsios, Climate, environment and cognition in the colonisation of the Eastern Mediterranean islands during the Pleistocene. *Quat. Int.* **577**, 1–14 (2021), 10.1016/j.quaint.2020.09.012.
17. O. Bar-Yosef, N. Goren-Inbar, The lithic assemblages of 'Ubeidiya: A Lower Palaeolithic site in the Jordan Valley. *Oesem* **34**, 1–266 (1993).
18. E. Tchernov, L. K. Horwitz, A. Ronen, A. Lister, The faunal remains from evron quarry in relation to other lower paleolithic hominid sites in the southern Levant. *Quat. Res.* **42**, 328–339 (1994), 10.1006/qres.1994.1083.
19. N. Goren-Inbar *et al.*, Pleistocene milestones on the out-of-Africa corridor at Geshen Benot Ya'aqov, Israel. *Science* **289**, 944–947 (2000), 10.1126/science.289.5481.944.
20. Y. Zaidner, R. Yeshurun, C. Mallol, Early Pleistocene hominins outside of Africa: Recent excavations at Bizat Ruhama, Israel. *PaleoAnthropol.* **2010**, 162–195 (2010), 10.4207/PA.2010.ART38.
21. R. Dennell, Dispersal and colonisation, long and short chronologies: How continuous is the Early Pleistocene record for hominids outside East Africa? *J. Hum. Evol.* **45**, 421–440 (2003), 10.1016/j.jhevol.2003.09.006.
22. S. P. E. Blockley, R. Pinhasi, A revised chronology for the adoption of agriculture in the Southern Levant and the role of Lateglacial climatic change. *Quat. Sci. Rev.* **30**, 98–108 (2011), 10.1016/j.quascirev.2010.09.021.
23. S. McGrail, *Boats of the World: From the Stone Age to Medieval Times* (Oxford University Press, Oxford, United Kingdom, 2004).
24. C. J. A. Bradshaw *et al.*, Minimum founding populations for the first peopling of Sahul. *Nat. Ecol. Evol.* **3**, 1057–1063 (2019), 10.1038/s41559-019-0902-6.
25. M. Krapp, R. M. Beyer, S. L. Edmundson, P. J. Valdes, A. Manica, A statistics-based reconstruction of high-resolution global terrestrial climate for the last 800,000 years. *Sci. Dat.* **8**, 228 (2021), 10.1038/s41597-021-01009-3.
26. P. J. Reimer *et al.*, The IntCal20 Northern Hemisphere radiocarbon age calibration curve (0–55 cal kBP). *Radiocarbon* **62**, 725–757 (2020), 10.1017/RDC.2020.41.
27. S. Herrando-Pérez, F. Saltré, Estimating extinction time using radiocarbon dates. *Quat. Geochronol.* **79**, 101489 (2023), <https://doi.org/10.1016/j.quageo.2023.101489>.
28. F. Saltré *et al.*, Climate-human interaction associated with southeast Australian megafauna extinction patterns. *Nat. Commun.* **10**, 5311 (2019), 10.1038/s41467-019-13277-0.
29. C. J. A. Bradshaw *et al.*, Directionally supervised cellular automaton for the initial peopling of Sahul. *Quat. Sci. Rev.* **303**, 107971 (2023), 10.1016/j.quascirev.2023.107971.
30. C. J. A. Bradshaw *et al.*, Stochastic models support rapid peopling of Late Pleistocene Sahul. *Nat. Commun.* **12**, 2440 (2021), 10.1038/s41467-021-21551-3.
31. A. Palmisano, A. Bevan, D. Lawrence, S. Shennan, The NERD dataset: Near east radiocarbon dates between 15,000 and 1,500 cal. yr BP. *J. Open Archaeol. Dat.* **10**, 2 (2022), 10.5334/joad.90.
32. L. A. Maher, People and their places at the End of the Pleistocene: Evaluating perspectives on physical and cultural landscape change (Council for British Research in the Levant, Oxbow Books, Oxford, United Kingdom, 2010), pp. 34–45.
33. C. G. Karydas, P. Panagos, Modelling monthly soil losses and sediment yields in Cyprus. *Intl. J. Dig. Earth* **9**, 766–787 (2016), 10.1080/17538947.2016.1156776.
34. A. Simmons, R. D. Mandel, "Site formation processes at Akrotiri Aetokremnos, Cyprus: Why is the site so controversial?" in *Géochronologie des Îles de Méditerranée*, M. Ghilardi, Ed. (CNRS Éditions, Paris, 2016), pp. 57–72.
35. J. Louys *et al.*, No evidence for widespread island extinctions after Pleistocene hominin arrival. *Proc. Natl. Acad. Sci. U.S.A.* **118**, e2023005118 (2021), 10.1073/pnas.2023005118.
36. A. J. Weaver, O. A. Saenko, P. U. Clark, J. X. Mitrovica, Meltwater Pulse 1A from Antarctica as a trigger of the Bolling-Allerød Warm Interval. *Science* **299**, 1709–1713 (2003), 10.1126/science.1081002.
37. D. A. Fordham *et al.*, PaleoView: A tool for generating continuous climate projections spanning the last 21,000 years at regional and global scales. *Geography* **40**, 1348–1358 (2017), 10.1111/egoc.03031.
38. A. Belfer-Cohen, A. N. Goring-Morris, Current issues in Levantine upper Palaeolithic research (Oxbow Books, Oxford, United Kingdom, 2003), pp. 1–12.
39. L. R. Binford, *Constructing Frames of Reference: An Analytical Method for Archaeological Theory Building Using Ethnographic and Environmental Data Sets* (University of California Press, Berkeley, 2001).
40. A. H. Simmons, "Faunal extinction in an Island society" in *Pygmy Hippopotamus Hunters of Cyprus (Interdisciplinary Contributions to Archaeology)*, Kluwer Academic/Plenum Publishers, New York, USA, 1999).
41. N. Efstratiou, D. Kyriakou, "Mountain archaeology in Cyprus between the two coasts: Past experience and future prospects" in *Four Decades of Hiatus in Archaeological Research in Cyprus: Towards Restoring the Balance*, D. Pilides, M. Mina, Eds. (Holhausen der Verlag, Vienna, Austria, 2017), pp. 56–65.
42. A. J. Ammerman, "Cyprus: The submerged final Palaeolithic of Aspros Dive Site C" in *The Archaeology of Europe's Drowned Landscapes*, G. Bailey, N. Galanidou, H. Peeters, H. Jöns, M. Mennenga, Eds. (Springer International Publishing, Cham, 2020), pp. 429–442.
43. M. Given, A. B. Knapp, *The Sydney Cyprus Survey Project: Social Approaches to Regional Archaeological Survey* (University of California Los Angeles, Los Angeles, California, USA, Cotsen Institute of Archaeology, 2003), vol. **21**.
44. C. McCartney, S. W. Manning, D. Sewell, S. T. Stewart, "Reconsidering early Holocene Cyprus within the eastern Mediterranean landscape" in *Landscapes in Transition*, B. Finlayson, G. Warren, Eds. (Oxbow Books, Oxford, United Kingdom, 2010), pp. 133–146.
45. S. T. Stewart *et al.*, Early Neolithic chert variability in central Cyprus: Geo-chemical and spatial analyses. *J. Archaeol. Sci. Rep.* **29**, 102088 (2020), 10.1016/j.jasrep.2019.102088.
46. J.-D. Vigne, F. Briois, J. Guilaine, Eds., *Klimonas. An Early Pre-Pottery Neolithic Village in Cyprus* (CNRS Éditions/Gallia Préhistoire, Paris, 2023).
47. H. J. Zahid, E. Robinson, R. L. Kelly, Agriculture, population growth, and statistical analysis of the radiocarbon record. *Proc. Natl. Acad. Sci. U.S.A.* **113**, 931–935 (2016), 10.1073/pnas.1517650112.
48. J. Luis Lanata, L. Martino, A. Osella, A. García-Herbst, Demographic conditions necessary to colonize new spaces: The case for early human dispersal in the Americas. *World Archaeol.* **40**, 520–537 (2008), 10.1080/00438240802452890.
49. V. V. Venkataraman, T. S. Kraft, N. J. Dominy, K. M. Endicott, Hunter-gatherer residential mobility and the marginal value of rainforest patches. *Proc. Natl. Acad. Sci. U.S.A.* **114**, 3097–3102 (2017), 10.1073/pnas.1617542114.
50. M. J. Hamilton, J. Lobo, E. Rupley, H. Yoon, G. B. West, The ecological and evolutionary energetics of hunter-gatherer residential mobility. *Evol. Anthropol. Iss. News Rev.* **25**, 124–132 (2016), 10.1002/evan.21485.
51. P. Roberts, B. A. Stewart, Defining the 'generalist specialist' niche for Pleistocene *Homo sapiens*. *Nat. Hum. Behav.* **2**, 542–550 (2018), 10.1038/s41562-018-0394-4.
52. P. Kyriakidis *et al.*, Virtual sea-drifting experiments between the Island of Cyprus and the surrounding mainland in the early prehistoric Eastern Mediterranean. *Heritage* **5**, 3081–3099 (2022), 10.3390/heritage5040160.
53. I. Hanski, Metapopulation dynamics. *Nature* **396**, 41–49 (1998), 10.1038/23876.
54. M. J. Hamilton, B. T. Milne, R. S. Walker, O. Burger, J. H. Brown, The complex structure of hunter-gatherer social networks. *Proc. R. Soc. Lond. B* **274**, 2195–2203 (2007), 10.1098/rspb.2007.0564.
55. P. M. Signor, J. H. Lipps, "Sampling bias, gradual extinction patterns, and catastrophes in the fossil record" in *Geological Implications of Impacts of Large Asteroids and Comets on the Earth*, L. T. Silver, P. H. Schultz, Eds. (Geological Society of America, Boulder, Colorado, 1982), pp. 291–296.
56. D. M. Raup, Biological extinction in Earth history. *Science* **231**, 1528–1533 (1986), 10.1126/science.11542058.
57. E. Tsakalos, N. Efstratiou, Y. Bassiakos, M. Kazantzaki, E. Filippaki, Early Cypriot prehistory: On the traces of the last hunters and gatherers on the island—Preliminary results of luminescence dating. *Curr. Anthropol.* **62**, 412–425 (2021), 10.1086/716100.
58. C. J. A. Bradshaw, A. Cooper, C. S. M. Turney, B. W. Brook, Robust estimates of extinction time in the geological record. *Quat. Sci. Rev.* **33**, 14–19 (2012), 10.1016/j.quascirev.2011.11.021.
59. F. Saltré *et al.*, Uncertainties in dating constrain model choice for inferring extinction time from fossil records. *Quat. Sci. Rev.* **112**, 128–137 (2015), 10.1016/j.quascirev.2015.01.022.
60. A. R. Solow, D. L. Roberts, K. M. Robbitt, On the Pleistocene extinctions of Alaskan mammoths and horses. *Proc. Natl. Acad. Sci. U.S.A.* **103**, 7351–7353 (2006), 10.1073/pnas.0509480103.
61. B. W. Silverman, *Density Estimation for Statistics and Data Analysis* (Chapman and Hall, London, 1986), p. 175.
62. K. Lambeck, H. Rouby, A. Purcell, Y. Sun, M. Sambridge, Sea level and global ice volumes from the Last Glacial Maximum to the Holocene. *Proc. Natl. Acad. Sci. U.S.A.* **111**, 15296–15303 (2014), 10.1073/pnas.1411762111.
63. C. J. A. Bradshaw, S. Herrando-Pérez, Logistic-growth models measuring density feedback are sensitive to population declines, but not fluctuating carrying capacity. *Ecol. Evol.* **13**, e10010 (2023), 10.1002/eece3.10010.
64. J. O. Kaplan *et al.*, Climate change and Arctic ecosystems: 2. Modeling, paleodata-model comparisons, and future projections. *J. Geophys. Res. Atmos.* **108**, 8171 (2003), 10.1029/2002JD002559.
65. Z. Liu *et al.*, Transient simulation of Last Deglaciation with a new mechanism for Bolling-Allerød warming. *Science* **325**, 310–314 (2009), 10.1126/science.1171041.
66. Z. Liu *et al.*, Evolution and forcing mechanisms of El Niño over the past 21,000 years. *Nature* **515**, 550–553 (2014), 10.1038/nature13963.
67. H. Goosse *et al.*, Description of the Earth system model of intermediate complexity LOVECLIM version 1.2. *Geosci. Mod. Dev.* **3**, 603–633 (2010), 10.5194/gmd-3-603-2010.
68. H. Cadd *et al.*, A continental perspective on the timing of environmental change during the last glacial stage in Australia. *Quat. Res.* **102**, 5–23 (2021), 10.1017/qua.2021.16.
69. M. Tallavaara, J. T. Eronen, M. Luoto, Productivity, biodiversity, and pathogens influence the global hunter-gatherer population density. *Proc. Natl. Acad. Sci. U.S.A.* **115**, 1232–1237 (2018), 10.1073/pnas.1715638115.
70. W. Siler, A competing-risk model for animal mortality. *Ecology* **60**, 750–757 (1979), 10.2307/1936612.
71. M. Gurven, H. Kaplan, Longevity among hunter-gatherers: A cross-cultural examination. *Pop. Dev. Rev.* **33**, 321–365 (2007), 10.1111/j.1728-4457.2007.00171.x.
72. R. Walker *et al.*, Growth rates and life histories in twenty-two small-scale societies. *Am. J. Hum. Biol.* **18**, 295–311 (2006), 10.1002/ajhb.20510.
73. G. R. Bentley, Hunter-gatherer energetics and fertility: A reassessment of the Kung San. *Hum. Ecol.* **13**, 79–109 (1985), 10.1007/BF01531090.
74. H. Caswell, *Matrix Population Models: Construction, Analysis, and Interpretation* (Sinauer Associates Inc, Sunderland, USA, ed. 2, 2001).
75. D. H. Reed, J. J. O'Grady, J. D. Ballou, R. Frankham, The frequency and severity of catastrophic die-offs in vertebrates. *Anim. Conserv.* **6**, 109–114 (2003), 10.1017/S13679430030147.
76. R. Frankham, C. J. A. Bradshaw, B. W. Brook, Genetics in conservation management: Revised recommendations for the 50/500 rules. *Red List criteria and population viability analyses. Biol. Conserv.* **170**, 56–63 (2014), 10.1016/j.biocon.2013.12.036.
77. C. J. A. Bradshaw, F. Saltré, *Bradshaw/CyprusHumanPleistocene: v2.0* (final version + DOI). Zenodo. <https://zenodo.org/records/10951688>. Deposited 10 April 2024.